Journal of Physics: Conference Series **205** (2010) 012010 doi:10.1088/1742-6596/205/1/012010

Covariant density functional theory beyond mean field and applications for nuclei far from stability

P Ring

Physics Department, Technical University of Munich, 85748 Garching, Germany

E-mail: ring@ph.tum.de

Abstract. Density functional theory provides a very powerful tool for a unified microscopic description of nuclei all over the periodic table. It is not only successful in reproducing bulk properties of nuclear ground states such as binding energies, radii, or deformation parameters, but it also allows the investigation of collective phenomena, such as giant resonances and rotational excitations. However, it is based on the mean field concept and therefore it has its limits. We discuss here two methods based based on covariant density functional theory going beyond the mean field concept, (i) models with an energy dependent self energy allowing the coupling to complex configurations and a quantitative description of the width of giant resonances and (ii) methods of configuration mixing between Slater determinants with different deformation and orientation providing are very successful description of transitional nuclei and quantum phase transitions.

1. Introduction

The structure of nuclei far from stability with extreme isospin is one the most exciting challenges of present nuclear physics. New experimental facilities with radioactive nuclear beams make it possible to investigate the nuclear chart to the very limits of nuclear binding. A wealth of structure phenomena in exotic nuclei have been reported and the next generation of radioactive-beam facilities will present new exciting opportunities to study not only the ground states but also excitations and spectra of these strongly interacting many-body systems. This situation has stimulated considerable new efforts on the theoretical side to understand the dynamics of the nuclear many-body problem by microscopic methods.

Density functional theory (DFT) provides a universal tool to provide a quantitative microscopic description for a large majority of nuclei. Considerable progress has been reported recently in constructing such functionals [1]. A very successful example is covariant density functional theory (CDFT) in the form of the Relativistic Hartree-Bogoliubov (RHB) model [2, 3, 4]. It combines a density dependence with pairing correlations based on an effective interaction of finite range.

In principle density functional theory can be used for the description of all properties depending on the single-particle density. It is therefore not only limited to the description of the ground state properties. The same density functionals have also been applied for a very successful description of excited states, such as rotational bands in normal and super-deformed nuclei [5, 6] and collective vibrations [7, 8, 9]. Relativistic RPA and QRPA provides a natural framework to investigate collective and non-collective excitations of ph- (or $2qp$) character. It is successful in particular for the understanding of the position of giant resonances. Recently it

has been also used for a theoretical interpretation of low lying E1-strengths observed in neutron rich isotopes (pygmy modes) [9] and for low-lying collective quadrupole excitations [10].

However, density functional theory in nuclei is based on intrinsic densities and on the mean field approach. Therefore it cannot provide an exact treatment of the full nuclear dynamics. It breaks down in several respects. We discuss here two examples of phenomena in nuclear structure, which cannot be described properly within this concept and we discuss methods based on CDFT to overcome these shortcomings: (i) the fact, that the self energy does not depend on energy, leads to pure single particle states, which are not coupled to more complex configurations and not fragmented as it is observed in experiment. In particular this theory does not provide the proper level density at the Fermi surface and the collective vibrations are only of *ph*-structure. The coupling the complex configurations is absent and therefore the width of giant resonances is not reproduced properly, (ii) conventional density functional theory breaks breaks also down in transitional nuclei, where the intrinsic density is not well defined and where one has to include correlations going beyond the mean field approximation by treating quantum fluctuations through a superposition of several mean field solutions, as for instance in the Generator Coordinate Method (GCM) [11].

2. Covariant density functional theory with complex configurations

The fact that DFT usually provides a poor approximation for the single-particle spectra, particularly for those of ideal shell model nuclei such as ^{208}Pb, is connected with the relatively small effective mass in such models. In finite nuclei the effective mass is influenced by the coupling to low-lying surface phonons. It leads to an energy dependent self energy. The single particle levels are then fragmented and shifted. These effects are not included in conventional DFT.

Already before density functional theory has been introduced in the sixties for the description of quantum mechanical many-body problems by Kohn and Sham [12] Landau has developed in the fifties his Fermi Liquid Theory [13] for infinite systems. It has been extended to the Theory of Finite Fermi Systems (TFFS) [14] by Migdal. This theory provides another very successful method for the description of low-lying nuclear excitations [15]. It has several general properties in common with density functional theory. First, both theories are know to be exact, at least in principle, but in practice, in nuclear physics, the parameters entering these theories have to be determined in a phenomenological way by adjustment to experimental data. Second, both theories are based on a single-particle concept. DFT uses the mean field concept with Slater determinants in an effective single-particle potential as a vehicle to introduce shell-effects in the exact density functional introduced by Hohenberg and Kohn [16]. Fermi liquid theory is based on the concept of quasi-particles obeying a Dyson equation, which are defined as the basic excitations of the neighboring system with odd particle number. Third, in practical applications both theories describe in the simplest versions the nuclear excitations in the RPA approximation, i.e. by a linear combination of *ph*-configurations in an average nuclear potential.

However, there are also essential differences between these two concepts. First, in contrast to DFT, TFFS does not attempt to calculate the ground state properties of the many-body system, but it describes the nuclear excitations in terms of Landau quasi-particles and their interaction. Therefore the experimental data used to fix the phenomenological parameters of the theories are bulk properties of the ground state in the case of density functional theory, and properties of single-particle excitations and of the collective excitations in the case of finite Fermi systems theory. Second, in DFT the mean field is determined in a self-consistent way and therefore the RPA spectrum contains Goldstone modes at zero energy. This is usually not the case in TFFS calculations, which are based on a non-relativistic shell-model potential, whose parameters are adjusted to the experimental single-particle spectra. Therefore, there is no self-consistency in the RPA calculations of TFFS and the Goldstone modes do not separate from the

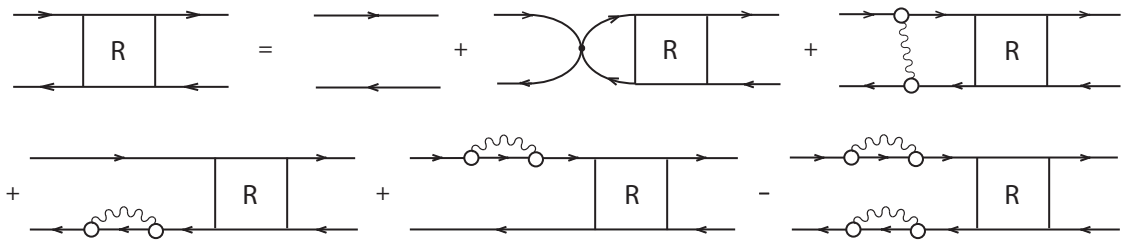

Figure 1. Bethe-Salpeter equation for the *ph*-response function R in graphical representation. Details are given in Fig. 1 and the small black circle means the static part of the residual *ph*-interaction V.

other modes. They are distributed among the low-lying excitations and have to be separated afterwards by special techniques. Third, modern versions of TFFS go much beyond the mean field approximation. The coupling between the particles and the phonons is investigated with Green's function techniques. Based on the phonons calculated in the framework of the RPA one has included particle-phonon coupling vertices and an energy dependence of the self-energy in the Dyson equation [17]. This leads also to an induced interaction in the Bethe-Salpeter equation caused by the exchange of phonons which also depends on the energy. The coupling of particles and phonons has also been derived from Nuclear Field Theory (NFT) and its extensions [18, 19].

Recently it has been attempted [20, 21, 22, 23] to find a combination of the basic ideas of covariant density functional theory and Landau-Migdal theory. The starting point is a covariant density functional $E[\rho]$ widely used in the literature, e.g. NL3 [24]. Without any additional parameter, it provides the necessary input of finite Fermi systems theory, such as the mean field and the single-particle spectrum as well as an effective interaction between the *ph*-configurations in terms of the second derivative of the same energy $E[\rho]$ with respect to the density. Thus the phenomenological input of Landau-Migdal theory is replaced by the results of density functional theory. The same interaction is used to calculate the vertices for particle-vibration coupling [20]. In a second step techniques of Landau-Migdal theory and its modern extensions are used to describe the coupling of one- and two-quasiparticle configurations. The main assumption of the quasiparticle-phonon coupling model is that two types of elementary excitations – two-quasiparticle and vibrational modes – are coupled in such a way that configurations of $1p1h \otimes phonon$ type with low-lying phonons strongly compete with simple $1p1h$ configurations close in energy or, in other words, that quasiparticles can emit and absorb phonons with rather high probabilities. In this way a fully consistent description of the many-body dynamics is obtained. As a result an induced additional interaction between single-particle and vibrational excitations provides a strong fragmentation of the pure RQRPA states causing the spreading width of giant resonances and the redistribution of the pygmy strength.

Nuclear dynamics of an even-even nucleus in a weak external field is described by the response function $R(14, 23)$, where This response function is the solution of the Bethe–Salpeter equation (BSE) in the *ph*-channel:

$$R(14,23) = R^0(14,23) - i \sum_{5678} R^0(16,25) W(58,67) R(74,83), \tag{1}$$

where R^0 is the free response and W is the effective *ph*-interaction obtained as the derivative of the self energy with respect to the density. Neglecting the energy dependent term in the self energy we obtain the linearized Bethe-Salpeter equation with the static interaction V as the second derivative of the energy density functional with respect to the density. This is conventional linear response or RPA theory. In addition to the static interaction V the

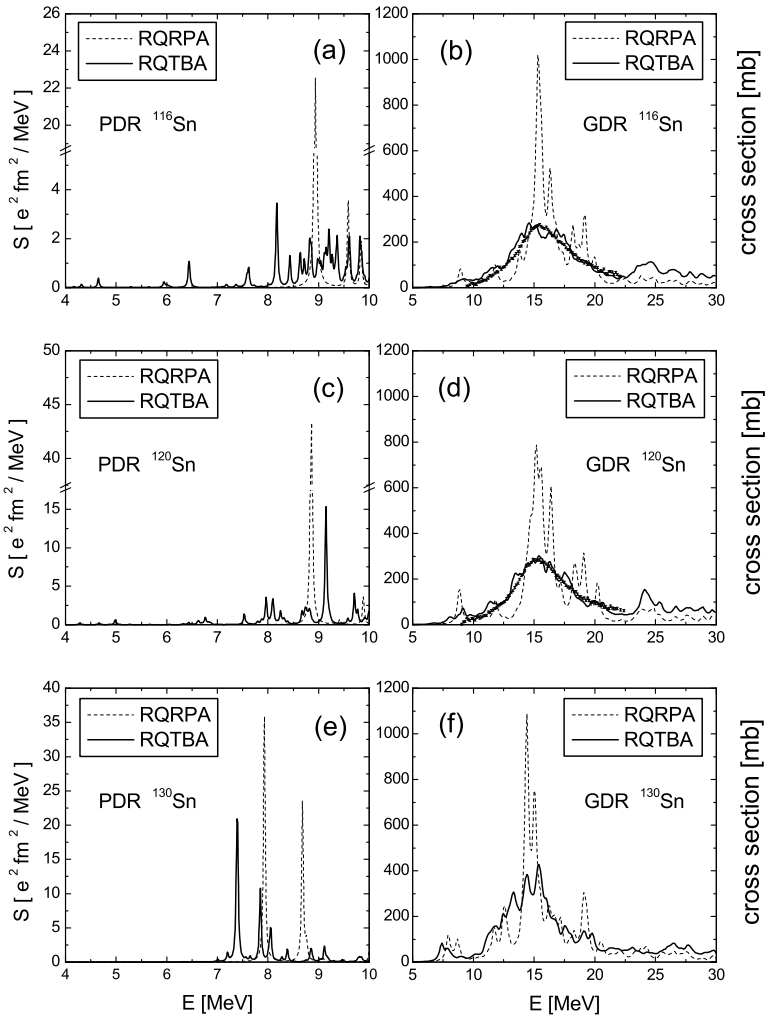

Figure 2. The calculated dipole spectra for the heavier tin isotopes ^{116}Sn, ^{120}Sn, ^{130}Sn, compared to data of Ref. [25] for ^{116,120}Sn. Right panels (b, d, f): photo absorption cross sections computed with the artificial width 200 keV. Left panels (a, c, e): the low-lying portions of the corresponding spectra in terms of the strength function, calculated with 20 keV smearing. Calculations within the RQRPA are shown by the dashed curves, and the RQTBA - by the solid curves.

effective interaction W contains terms derived from the energy dependent part of the self-energy. They contain diagrams with energy-dependent self-energies and an energy-dependent *induced interaction*, where a phonon is exchanged between the particle and the hole as shown in Fig. 1

To describe the observed spectrum of the excited nucleus in a weak external field D, as for instance a dipole field, one needs to calculate the strength function

$$S_D(E) = -\frac{1}{\pi}\mathrm{Im}\left(D^\dagger R((E))D\right)., \tag{2}$$

In Fig. 2 we show dipole spectra for the tin isotopes ^{116}Sn, ^{120}Sn, ^{130}Sn. The right panels show the photoabsorption cross section derived from the dipole strength function S_D. The left

panels show the low-lying parts of the corresponding spectrum in terms of the strength function. A small imaginary part of 20 keV is used for the energy variable, in order to see the fine structure of the spectrum and sometimes individual levels in this region. RQRPA calculations are shown by dashed curves and the RQTBA by the solid curves. Experimental data are taken from the EXFOR database [25].

These figures clearly demonstrate how the two-quasiparticle states, which are responsible for the spectrum of the RQRPA excitations, are fragmented through the coupling to the collective vibrational states. The effect of the particle-vibration coupling on the low-lying dipole strength below and around the neutron threshold within the presented approach is shown in the left panels of the Fig. 2. Such calculations give us an example how the low-lying strength develops with the increase of the neutron excess. It is also found that the presence of pairing correlations causes a noticeably stronger fragmentation of both the GDR and the PDR modes as compared to the case of a normal system. This effect has the two reasons. First, pairing correlations lead to a diffuseness of the Fermi surface and, thus, increase the number of possible $2qp \otimes phonon$ configurations, and second, pairing correlations cause a considerable lowering of the energies and increased transition probabilities of the lowest 2^+ states. In spherical open-shell medium mass nuclei the highly collective first 2^+ states appear at energies around 1 MeV (and they are usually well reproduced in RQRPA calculations [26]) whereas in magic nuclei and often in nuclei near the shell closures they appear much higher, at about 3-4 MeV and have considerably reduced transition probabilities. This causes a strong configuration mixing in the case of presence of very low-lying vibrational states.

A systematic analysis of the transition densities of the RQRPA and the RQTBA states shows that the $2qp$ transition densities in the broad low-lying energy region dominated by the fragmentation of the RQRPA pygmy mode have a very similar behavior as the initial RQRPA state: proton and neutron components oscillate in phase in the nuclear interior and neutron components dominate on the surface in nuclei with noticeable neutron excess.

3. Shape fluctuations in transitional nuclei

An important area, where conventional density functional theory based on the mean field concept breaks down is the region of transitional nuclei. In this case it is not possible to define an intrinsic deformation of the system. In fact, in such cases the potential energy surfaces (PES) as a function of the deformation parameters are rather flat and many configurations with different deformations have nearly the same energy. One has to take into account fluctuations in deformation space by forming a superposition of wave functions with different deformation.

In the following we study as an example the effects of quantum fluctuation for triaxial shapes in the nucleus ^{16}C. First we generate a set of deformed intrinsic wave functions $|q\rangle$ with the quadrupole deformations $q = (\beta, \gamma)$ generated by constrained RMF+BCS calculations. Of course, for all the non-spherical points with $(\beta \neq 0)$ the intrinsic wave functions $|\beta \neq 0, \gamma\rangle$ have a certain orientation and rotational symmetry is broken. To restore this symmetry, a three-dimensional angular momentum projection (3DAMP) [27] is carried out. The left panel of Fig. 3 shows the unprojected (MF) and the J-projected ($J^\pi = 0^+$) energy surfaces in the β-γ plane.

As found already in the eighties [30] we observe in the J-projected surface a triaxial minimum This minimum is still very soft along the γ direction. One has, therefore, to allow for superpositions of wave functions with different deformations and to perform a GCM calculation in the full β-γ plane

$$|\Psi^J_M\rangle = \sum_K \int d^2q f_K(q) P^J_{MK} |q\rangle \tag{3}$$

including correlations due to restoration of broken symmetries and fluctuations of the deformation coordinates. The weight function $f(q)$ is determined by the solution of the Hill

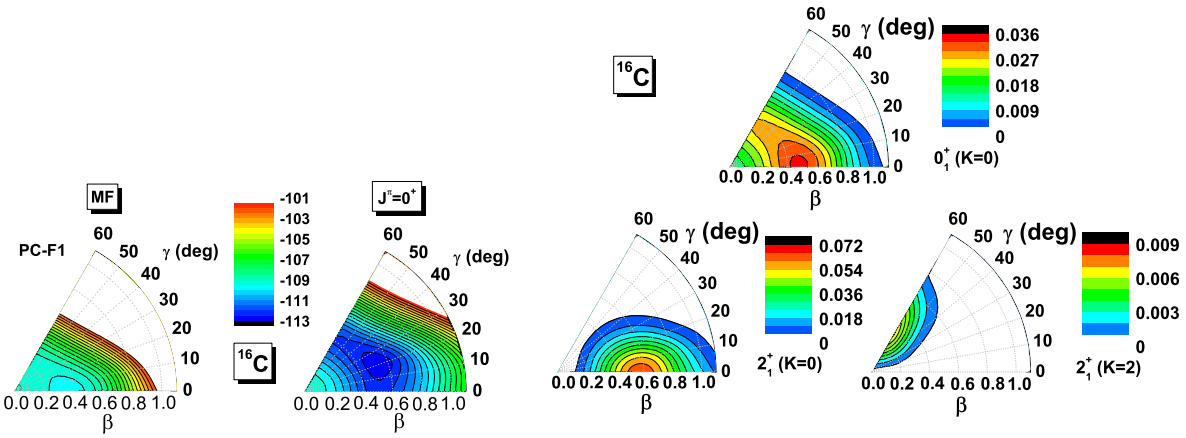

Figure 3. Left panel: Potential energy surfaces in β-γ plane for the nucleus ^{16}C obtained by triaxial relativistic mean-field calculations (MF) and with projection onto angular momentum after the variation ($J^\pi = 0^+$). Right panel: Contour plots of the probability distributions in β and γ from 3DAMP+GCM calculation for the ground state (0_1^+) and the first excited state (2_1^+)

Wheeler equation [11].

The right panel of Fig. 3 shows contour plots of the probability distributions derived from $f(q)$ in the β-γ plane resulting from 3DAMP+GCM calculations for both the ground state (0_1^+) and the first excited state (2_1^+). The ground state has a triaxial structure with almost uniform probability along the γ-direction which indicates an obvious quantum shape fluctuation in γ direction. For $J = 2$ we have K-mixing and we therefore show the two distributions for $K = 0$ and $K = 2$ separately. Both are concentrated along the axially symmetric configurations with $K = 0$ on the prolate and $K = 2$ on the oblate side. However, the $K = 0$ part exhausts 93.1% of the norm so that the nucleus has a strong prolate deformation in the (2_1^+) state with $\beta \simeq 0.6$.

To show the importance of shape fluctuations in γ for spectroscopic properties, we plot in

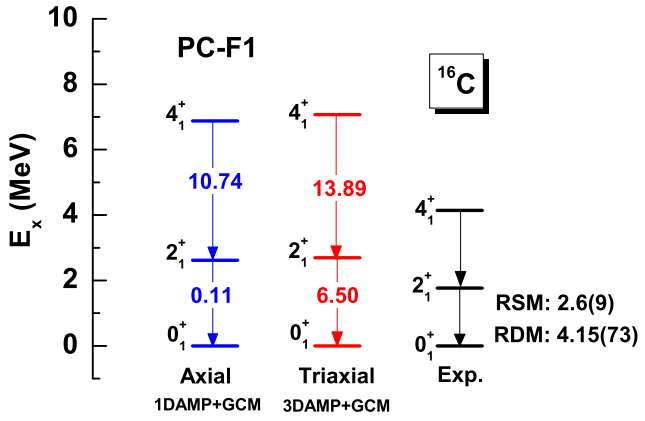

Figure 4. (Color online) The lowest energy levels of angular momentum $J = 0, 2, 4$ in ^{16}C. The $B(E2)$ values are in units of e^{2}fm^4. The experimental data are taken from Refs. [28, 29].

Fig. 4 the lowest energy levels with $J = 0, 2, 4$ obtained from the 1DAMP+GCM, where only axial symmetric configuratons $\gamma = 0$ are superimposed for various β-values and 3DAMP+GCM calculations and compare them with experiment [29]. The inclusion of triaxial states does not change the energy spectrum too much, but it improves the electric quadrupole transitions significantly. Only with a proper treatment of the shape fluctuations in γ, are the calculated $B(E2 : 2_1^+ \rightarrow 0_1^+) = 6.50$ e^{2}fm^4 in agreement with recent data.

The predicted ratio $R_{4/2} \equiv E_4/E_2 = 2.63$ is a little larger than the experimental value $R_{4/2} = 2.35$. Both are close to the $R_{4/2} = 2.50$, a typical value for γ-soft nuclei. The predicted deviations of $R_{4/2}$ from experiment go in the direction of a rotor ($R_{4/2} = 3$). As observed in many calculations using projection after variation [31, 32, 33, 34] the calculated spectrum is systematically stretched. It would be far more compressed by the inclusion of a cranking term in the mean-field calculation [5].

Acknowledgments

I am very grateful to all my collaborators participating in the work presented here, in particular to E. Litvinova, J. Meng, V. Tselyaev, and J.M. Yao. This work was supported in part by the DFG cluster of excellence "Origin and Structure of the Universe" (www.universe-cluster.de).

References

[1] Bender M, Heenen P H and Reinhard P G 2003 *Rev. Mod. Phys.* **75** 121
[2] Gonzales-Llarena T, Egido J L, Lalazissis G A and Ring P 1996 *Phys. Lett.* **379** 13
[3] Ring P 1996 *Prog. Part. Nucl. Phys.* **37** 193
[4] Vretenar D, Afanasjev A V, Lalazissis G A and Ring P 2005 *Phys. Rep.* **409** 101
[5] Afanasjev A V, König J, Ring P, Egido J L and Robledo L M 2000 *Phys. Rev.* C **62** 054306
[6] Afanasjev A V, Ring P and König J 2000 *Nucl. Phys.* A **676** 196
[7] Ring P, Ma Z Y, Giai N V, Vretenar D, Wandelt A and Cao L G 2001 *Nucl. Phys.* A **694** 249
[8] Ma Z Y, Wandelt A, Giai N V, Vretenar D, Ring P and Cao L 2002 *Nucl. Phys.* A **703** 222
[9] Paar N, Ring P, Nikšić T and Vretenar D 2003 *Phys. Rev.* C **67** 034312
[10] Ansari A 2005 *Phys. Lett.* B **623** 37
[11] Ring P and Schuck P 1980 *The Nuclear Many-Body Problem* (Berlin: Springer-Verlag)
[12] Kohn W and Sham L J 1965 *Phys. Rev.* **137** A1697
[13] Landau L D 1959 *Sov. Phys. JETP* **8** 70
[14] Migdal A B 1967 *Theory of Finite Fermi Systems: Applications to Atomic Nuclei* (New York: Wilson)
[15] Ring P and Speth J 1974 *Nucl. Phys.* A **235** 315
[16] Hohenberg P and Kohn W 1964 *Phys. Rev.* **136** B864
[17] Ring P and Werner E 1973 *Nucl. Phys.* A **211** 198
[18] Bohr A and Mottelson B 1975 *Nuclear Structure* vol II (Reading,Mass.: Benjamin)
[19] Bertsch G F, Bortignon P F and Broglia R A 1983 *Rev. Mod. Phys.* **55** 287
[20] Litvinova E and Ring P 2006 *Phys. Rev.* C **73** 044328
[21] Litvinova E, Ring P and Tselyaev V I 2007 *Phys. Rev.* C **75** 064308
[22] Litvinova E, Ring P and Tselyaev V I 2008 *Phys. Rev.* C **78** 014312
[23] Litvinova E, Ring P and Tselyaev V I 2009 *Phys. Rev.* C **79** 054312
[24] Lalazissis G A, König J and Ring P 1997 *Phys. Rev.* C **55** 540
[25] Experimental nuclear reaction data URL `http://www-nds.iaea.or.at/exfor/exfor00.htm`
[26] Ansari A and Ring P 2006 *Phys. Rev.* C **74** 054313
[27] Yao J M, Meng J, Ring P and Peña Arteaga D 2009 *Phys. Rev.* C **79** 044312
[28] Ong H J *et al.* 2008 *Phys. Rev.* C **78** 014308
[29] Wiedeking M *et al.* 2008 *Phys. Rev. Lett.* **100** 152501
[30] Hayashi A, Hara K and Ring P 1984 *Phys. Rev. Lett.* **53** 337
[31] Valor P and Bonche P 2000 *Nucl. Phys.* A **671** 145
[32] Bender M, Heenen P H and Reinhard P G 2003 *Rev. Mod. Phys.* **75** 121
[33] Rodríguez-Guzmán R, Egido J L and Robledo L M 2002 *Nucl. Phys.* A **709** 201
[34] Nikšić T, Vretenar D and Ring P 2006 *Phys. Rev.* C **73** 034308